

# Neuronal Shp2 tyrosine phosphatase controls energy balance and metabolism

Eric E. Zhang\*<sup>†</sup>, Emilie Chapeau\*, Kazuki Hagihara\*, and Gen-Sheng Feng\*<sup>††</sup>

\*Program in Signal Transduction, The Burnham Institute, 10901 North Torrey Pines Road, La Jolla, CA 92037; and <sup>†</sup>Molecular Pathology Graduate Program, University of California at San Diego, La Jolla, CA 92093

Edited by Jack E. Dixon, University of California at San Diego, La Jolla, CA, and approved September 30, 2004 (received for review July 13, 2004)

**Shp2, a Src homology 2-containing tyrosine phosphatase, has been implicated in a variety of growth factor or cytokine signaling pathways. However, it is conceivable that this enzyme acts predominantly in one pathway versus the others in a cell, depending on the cellular context. To determine the putative functions of Shp2 in the adult brain, we selectively deleted Shp2 in postmitotic forebrain neurons by crossing CaMKII $\alpha$ -Cre transgenic mice with a conditional Shp2 mutant (Shp2<sup>flox</sup>) strain. Surprisingly, a prominent phenotype of the mutant (CaMKII $\alpha$ -Cre:Shp2<sup>flox/flox</sup> or CaSKO) mice was the development of early-onset obesity, with increased serum levels of leptin, insulin, glucose, and triglycerides. The mutant mice were not hyperphagic but developed enlarged and steatotic liver. Consistent with previous *in vitro* data, we found that Shp2 down-regulates Jak2/Stat3 (signal transducer and activator of transcription 3) activation by leptin in the hypothalamus. However, Jak2/Stat3 down-regulation is offset by a dominant Shp2 promotion of the leptin-stimulated Erk pathway, leading to induction rather than suppression of leptin resistance upon Shp2 deletion in the brain. Collectively, these results suggest that a primary function of Shp2 in postmitotic forebrain neurons is to control energy balance and metabolism, and that this phosphatase is a critical signaling component of leptin receptor ObRb in the hypothalamus. Shp2 shows potential as a neuronal target for pharmaceutical sensitization of obese patients to leptin action.**

cell signaling | obesity | diabetes

Shp2 is a widely expressed cytoplasmic tyrosine phosphatase with two Src homology 2 domains that has attracted much attention in the cell signaling field in the past decade. Previous *in vitro* data from us and other groups have suggested possible involvement of Shp2 in signaling events initiated by a number of growth factors and cytokines (1, 2). However, there are two important issues that remain to be addressed. First, it is not clear yet whether this tyrosine phosphatase acts equally in many pathways in all cell types *in vivo* or whether it has a primary function in one pathway in a given cell type. Second, the physiological significance of many *in vitro* observations has yet to be determined. The critical issue now is to figure out how Shp2 operates in various cell types or at different developmental stages in mammals. Homozygous disruption of the *Shp2* gene resulted in embryonic lethality at mid-gestation in mice (3), which precluded further analysis of Shp2 activities in adult animals. Accordingly, we have used the cre-loxP system to create a conditional Shp2 mutant allele in mice, which allows us to dissect specific Shp2 functions in a differentiated cell type, such as a neuron.

Identification of leptin and its receptor has greatly advanced the knowledge for physiological control of energy balance and obesity (4, 5). Secreted by adipocytes, leptin activates the leptin receptor long form (ObRb) in the hypothalamus to control food intake, metabolism, and neuroendocrine responses to nutritional alteration (4, 6). However, the mechanism for leptin signaling through ObRb in the hypothalamus is poorly understood. Apart from its anorectic effect, the distinct metabolic action of leptin remains to be elucidated (7). *In vitro* biochemical data have suggested involvement of Shp2 and Stat3 (signal transducer and activator of transcription 3)

in proximal signaling events downstream of ObRb. Shp2 and Stat3 physically associate with leptin-activated ObRb by docking on the phosphorylated tyrosine residues, pY985 and pY1138, respectively (8–11). Several lines of evidence strongly support a major role of Stat3 in leptin signal relay in the hypothalamus. Intraperitoneal administration of leptin specifically activated Stat3 in the hypothalamus (12), and disruption of the ObRb–Stat3 interaction by introducing a Y-to-S mutation on the Stat3 binding site Y1138 caused leptin resistance and obesity in the knockin mice (13). A more recent report indicated that neural-specific Stat3 knockout (KO) (*Stat3<sup>N-/-</sup>*) mice developed obesity and recapitulated the abnormal phenotypes of *ob/ob* and *db/db* mice that are deficient in leptin and its receptor, respectively (14). Together, these data clearly defined a functional requirement for Stat3 in leptin control of energy balance. In contrast, the physiological significance of Shp2 action, if any, in leptin signaling remains to be elucidated, although the down-regulatory effect of Shp2 on leptin-induced Jak2 or Stat3 activity *in vitro* predicted that deletion of Shp2 would possibly overcome leptin resistance or enhance leptin signals (8, 9). We have created a mouse model in which Shp2 is selectively ablated in postmitotic neurons in the CNS, which unexpectedly leads to revelation of a critical role for Shp2 in control of energy balance and leptin signaling.

## Materials and Methods

**Generation of Shp2<sup>flox</sup> Allele and Brain-Specific Shp2 KO Mice.** To generate a conditional Shp2<sup>flox</sup> mutant allele, we engineered a targeting construct, with neomycin-resistance (*neo<sup>R</sup>*), thymidine kinase (TK), and diphtheria toxin (DT-A) genes as selective markers (Fig. 1A). R1 embryonic stem (ES) cells were transfected with the linearized targeting construct by electroporation and selected in DMEM containing G418 for homologous recombination. PCR analysis was used for screening of ES cell clones. Southern blot analysis identified ES clones with homologous recombination at the left and right arms (Fig. 1B). A correctly targeted ES cell clone was transfected with a Cre expression plasmid (pBS185) by electroporation and selected with 1-(2-deoxy-2-fluoro-D-arabino-furano-5-iodouracil (FIAU), to remove the *neo*-TK cassette. Three ES cell clones with a loxP-flxed Shp2 allele (Shp2<sup>flox</sup>) were injected into blastocysts to generate chimeric mice, and germ-line transmission of the Shp2<sup>flox</sup> allele was achieved from all three clones injected and backcrossed with C57BL/6 for at least three generations. Shp2<sup>flox/+</sup> mice were subsequently bred for two generations with CaMKII $\alpha$ -Cre transgenic mice (strain R1ag5) in the C57BL/6 background (15, 16). For Rosa26 reporter assay, CaMKII $\alpha$ -Cre mice were crossed with transgenic mice [B6.129S4-Gt(ROSA)26Sortm1Sor/J] from The Jackson Laboratory (17). In this study, Shp2<sup>flox/flox</sup> mice were used as WT

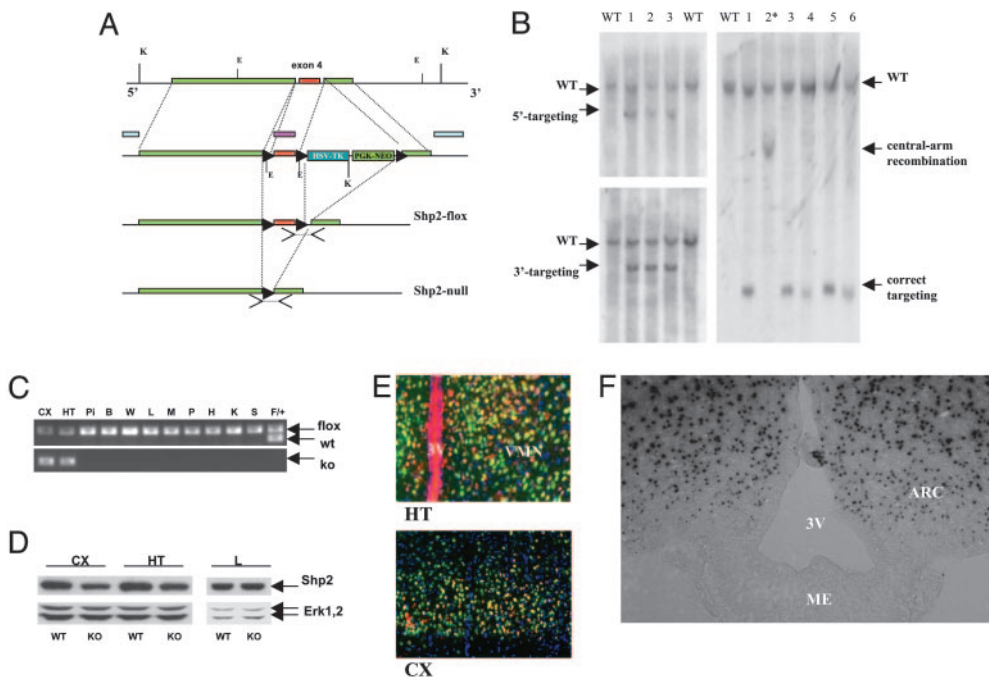
This paper was submitted directly (Track II) to the PNAS office.

Abbreviations: KO, knockout; Stat3, signal transducer and activator of transcription 3; ES, embryonic stem; GH, growth hormone; Pn, postnatal day *n*; BDNF, brain-derived neurotrophic factor.

<sup>†</sup>To whom correspondence should be addressed. E-mail: gfeng@burnham.org.

© 2004 by The National Academy of Sciences of the USA

**Fig. 1.** Generation of neuronal-specific Shp2 KO mice. (A) The gene targeting strategy is shown together with the detection of PCR and Southern blot. To detect the *Shp2<sup>fllox</sup>* allele, a forward primer (5'-ACG TCA TGA TCC GCT GTC AG-3') in exon 4 and a reverse primer (5'-ATG GGA GGG ACA GTG CAG TG-3') in intron 4 were used. For the *Shp2<sup>null</sup>* allele, a forward primer (5'-CAG TTG CAA CTT TCT TAC CTC-3') in intron 3 and a reverse primer (5'-GCA GGA GAC TGC AGC TCA GTG ATG-3') within intron 4 were used. For Southern blot analysis, both 5' and 3' external probes were used as shown. In addition, a probe for the central arm was used for detection of unwanted central-arm recombinants. (B) Southern blot analysis of positive ES cell clones. Genomic DNA from ES cells was digested with *KpnI* and hybridized with the 5' or 3' external probes. WT allele displayed a 15-kb fragment with either the 5' or the 3' probe, whereas a correctly targeted allele exhibited a 9-kb band for the 5' probe and a 10-kb band for the 3' probe. After DNA digestion with *EcoRI*, the central arm probe detected a 7.8-kb band for the WT allele and a 0.8-kb band for a correctly targeted allele or a 3.4-kb band for a central-arm recombinant, as shown in lane 2\*.



(C) PCR analysis of various tissue samples from a CaSKO mouse at P28. The Cre-mediated DNA recombination was restricted to cerebral cortex (CX) and hypothalamus (HT) in the brain, as revealed by detection of the *Shp2* KO allele in these two areas only. Pi, pituitary gland; B, brown adipose tissue; W, white adipose tissues; L, liver; M, muscle; P, pancreas; H, heart; K, kidney; S, spleen. The *Shp2<sup>fllox</sup>* allele remained intact in nonneuronal cells. Tail DNA from a littermate (F/+) was included as a control. (D) Immunoblot analysis of lysates derived from cerebral cortex (CX), hypothalamus (HT), and liver (L), using a specific anti-Shp2 antibody. The Shp2 protein amounts in cerebral cortex and hypothalamus of CaSKO mice (KO) were reduced by 50–70% at P21, compared to littermate control (WT). The filter was stripped and reblotted with an anti-Erk1/2 antibody for loading control. (E) Double immunohistochemical staining of Cre (red) and NeuN (green) confirmed the restricted expression of Cre to neuronal cells in cerebral cortex and hypothalamus. The 4',6'-diamidino-2-phenylindole staining (blue) indicates the nonneuronal cells. 3V, third ventricle; VMN, ventromedial nucleus. (F) 5-Bromo-4-chloro-3-indolyl  $\beta$ -D-galactoside staining of hypothalamic section derived from CaMKII $\alpha$ -Cre:Rosa26 mice at P28. 3V, third ventricle; ME, median eminence; ARC, arcuate nucleus. (Magnifications: 200  $\mu$ M, E; 100  $\mu$ M, F.)

controls, Cre/+;Shp2<sup>fllox/+</sup> mice were used as heterozygous mutants, and Cre/+;Shp2<sup>fllox/fllox</sup> (CaSKO) mice were used as homozygous mutants.

**Phenotypic Analysis.** For measurement of mouse body weights, food intake, and anatomical analyses, data were collected daily between 10 a.m. and 12 p.m. For hormone studies, mouse sera were collected restrictively from 10 a.m. to 11 a.m. Blood glucose was determined on whole venous blood by using an automatic glucometer (One Touch Basic, Lifescan, Mountain View, CA). The serum leptin/insulin measurements were conducted by ELISA (Crystal Chem, Downers Grove, IL); corticosterone analysis was done by enzyme immunoassay (R & D Systems); cortisol, triiodothyronine, and thyroxine analysis was done by RIA (University of California at San Diego Hillcrest Medical Center), and thyroid-stimulating hormone and growth hormone (GH) analysis was done by RIA (University of California Los Angeles Harbor Medical Center). Serum triglyceride was determined by the diagnostic laboratory of the University of California at San Diego Animal Care Program. Except for mice in breeding or behavior examination, all mice analyzed were single-housed after weaning at postnatal day 21 (P21). All animal procedures were approved by The Burnham Institutional Animal Care and Use Committee.

**Molecular Signaling.** Polyclonal antibodies against ObRb protein and to phosphorylated Tyr-985 (pY985) of ObRb were from Alpha Diagnostic International, San Antonio, TX. Other antibodies used were polyclonal antibodies against the C-terminal tail of Shp2 (Santa Cruz Biotechnology), phospho-Erk1/2 or Erk1/2 kinases, phospho-tyrosyl (pY)-Stat3, Stat3, and pY-Jak2 (Cell Signaling Technology, Beverly, MA), Cre recombinase (Novagen), and a

mAb against NeuN (Chemicon). The secondary antibodies used in immunostaining were Alexa Fluor594 anti-rabbit IgG and Alexa Fluor488 anti-mouse IgG (1:200 dilution, Molecular Probes). Reagents for Oil-red-O and periodic acid-Schiff staining were from PolyScientific, Blacksburg, VA, and reagents for 5-bromo-4-chloro-3-indolyl  $\beta$ -D-galactoside staining were from Sigma. Recombinant mouse leptin was from the National Hormone and Peptide Program, Torrance, CA. For Northern blot, liver RNA was extracted by Trizol reagent (Invitrogen). For real-time RT-PCR, hypothalamic RNA was extracted by RNeasy kits (Qiagen, Valencia, CA), and the reaction was performed by LightCycler machine (Roche Applied Science) with a SYBR green RT-PCR kit (Qiagen). All results were presented as comparative analysis for littermates of control and CaSKO mice.

## Results

**Deletion of Shp2 in Forebrain Neurons Results in Obesity and Leptin Resistance in Mice.** To define the Shp2 functions in various cell types of adult animals, we created a conditional *Shp2* mutant (*Shp2<sup>fllox</sup>*) allele by introducing two *loxP* sites into introns flanking exon 4, which codes for amino acid residues 111–176 (Fig. 1 A and B). Deletion of exon 4 introduces a frame-shift mutation, creating an immediate stop codon. By crossing *Shp2<sup>fllox/fllox</sup>* mice with CaMKII $\alpha$ -Cre transgenic animals (15), we generated brain-specific Shp2 KO (CaMKII $\alpha$ -Cre:Shp2<sup>fllox/fllox</sup> or CaSKO) mice. Previous data showed that in the CaMKII $\alpha$ -Cre line Cre recombinase was expressed in postmitotic neuronal but not glial cells after P5 (16). PCR analysis confirmed a Cre-mediated specific recombination of the *Shp2<sup>fllox</sup>* allele in neuronal cells of cerebral cortex and hypothalamus, but not in other tissues (Fig. 1C). Immunoblot analysis using a specific anti-Shp2 antibody dem-

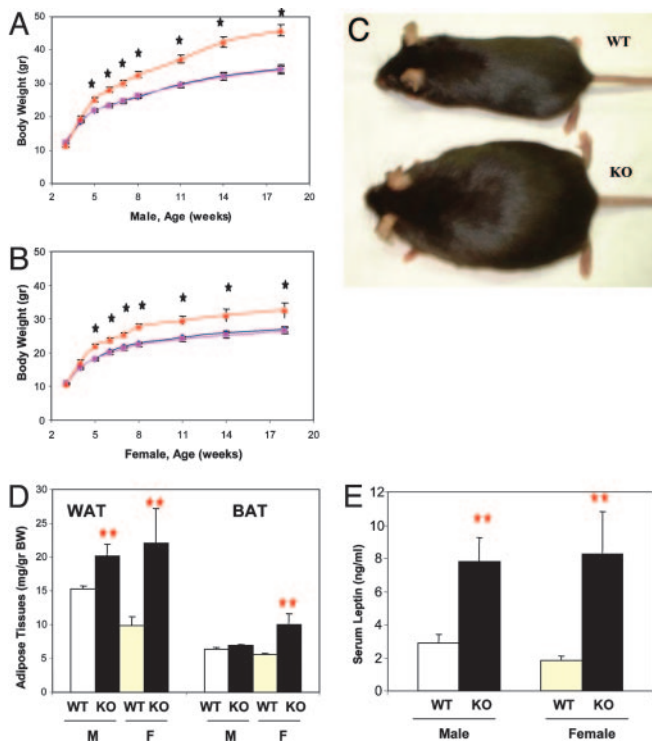


**Fig. 2.** CaSKO mice are obese and hyperleptinemic. (A and B) Body weights of CaSKO and control mice were measured at the indicated time points. Data are expressed as the means with SEM of at least 12 mice of each gender and genotype. Starting from P32 in males and P28 in females, there were significant differences between the CaSKO mice and controls/heterozygotes ( $P < 0.01$  in an unpaired Student's *t* test). WT (+/+, F/F; black diamond); heterozygous mice (Cre, F/+; pink square); CaSKO (Cre, F/F; red triangle). (C) Shown are two female littermates, a CaSKO (KO) and a control (WT), at 6 months. (D) White and brown adipose tissue (WAT and BAT, respectively) mass was assessed in mice at 8 weeks. Data represent the mean  $\pm$  SEM of at least eight mice of each gender (M, male; F, female) and genotype (\*\*,  $P < 0.01$ ). (E) Mouse serum samples were collected at 8 weeks, and leptin concentrations were determined by ELISA. Data represent the mean  $\pm$  SEM of at least eight mice of each gender (M, male; F, female) and genotype (\*\*,  $P < 0.01$ ).

onstrated a decrease by 50–70% of total Shp2 protein levels in lysates derived from hypothalamus and cerebral cortex of CaSKO mice at P21 (Fig. 1D). Double immunohistochemical staining of Cre and NeuN confirmed Cre expression in neuronal cells in hypothalamus and cerebral cortex (Fig. 1E). Rosa26 reporter assay in mice at P28 also indicated efficient Cre activity

in the arcuate nucleus of hypothalamus in CaMKII $\alpha$ -Cre mice (Fig. 1F).

Deletion of Shp2 did not cause defects in brain development, and the CaSKO mice appeared normal before weaning, apparently because CaMKII $\alpha$ -Cre-mediated gene recombination occurred mainly after P5 when the neural circuit was already established. Surprisingly, the immediately noticeable phenotype of CaSKO mice after weaning was an early-onset obesity and accelerated increase of body weight in both males and females, whereas heterozygous animals appeared normal (Fig. 2A–C). At 8 weeks of age, male and female mutant animals gained 28% and 21%, respectively, more weight than their WT and heterozygous littermates ( $P < 0.0001$ ). Overall, both male and female CaSKO adult mice weighed  $\approx$ 30–50% more than their age- and sex-matched littermates when fed regular chow food, and some older CaSKO mice even had body weight 100% more than the controls. The abnormal increase in body weight correlated with the development of early-onset obesity in CaSKO mice. At 8 weeks of age, male mutants had 32% more white adipose tissue than controls, whereas females had 123% more ( $P < 0.01$ , Fig. 2D). Similarly, females had 80% more brown adipose tissue ( $P < 0.01$ ), whereas males had 9% more ( $P = 0.184$ ). Consistent with the increase in fat tissue, serum triglyceride levels were significantly higher in mutants, with nearly 20% more in both males and females ( $P < 0.05$  each, Table 1). Notably, the serum leptin levels in CaSKO mice were significantly increased by 2.7-fold in the males and 4.6-fold in the females ( $P < 0.01$  each, Fig. 2E), suggesting a resistance to leptin.

Development of obesity in CaSKO mice is unlikely to be triggered by a direct interference of insulin signaling upon deletion of Shp2 in neuronal cells, as prior studies showed a distinctly different phenotype in neural-specific insulin receptor KO (NIRKO) mice (18). These NIRKO mice, fed regular chow diet, exhibited normal body weight within 6 months for males, with only a modest 10% increase in female body weight (18). Deletion of brain-derived neurotrophic factor (BDNF) in the postnatal brain also caused obesity and energy imbalance (16, 19, 20). We measured the expression levels of *BDNF* mRNA in the hypothalamus and found no difference between control and CaSKO mice (Fig. 6, which is published as supporting information on the PNAS web site). Further functional analysis is required to determine whether deletion of Shp2 in the brain leads to development of resistance to BDNF.

**Neuronal-Specific Ablation of Shp2 Alters Leptin Signals in the Hypothalamus.** We then determined whether the obese and hyperleptinemic phenotype of CaSKO mice is associated with direct suppression of leptin signals in the hypothalamus. As shown in Fig. 3A, ObRb was coimmunoprecipitated with Shp2 in hypothalamic lysates prepared from WT mice after i.p. injection of leptin for 15

**Table 1. Phenotypic characterization of CaSKO mice**

	Genotype			P value (control vs. KO)
	F/F	F/+, Cre	F/F, Cre	
Weight (male), g*	27.1 $\pm$ 0.5	26.9 $\pm$ 0.6	34.5 $\pm$ 1.4	0.0002
Weight (female), g†	23.2 $\pm$ 0.5	22.8 $\pm$ 0.5	27.9 $\pm$ 1.3	0.001
Feeding, g per animal*	5.0 $\pm$ 0.2	4.9 $\pm$ 0.4	5.7 $\pm$ 1.4	0.184
Serum triglycerides	146.0 $\pm$ 9.3	ND	173.6 $\pm$ 7.3	0.039
Serum triglycerides	81.9 $\pm$ 3.6	ND	97.9 $\pm$ 7.0	0.047
Snout-anus length, mm*	91 $\pm$ 1	90 $\pm$ 1	98 $\pm$ 1	0.002
Body temperature‡	36.5 $\pm$ 0.2	ND	35.8 $\pm$ 0.2	0.019
Fertility (female)†	10/10 (100%)	20/20	8/12 (45%)§	NA

ND, not done; NA, not available.

\*8-week-old male mice.

†8-week-old females.

‡10-week-old males.

§For 3 months, 8 of 12 female KO mice delivered pups, and the average litter number was 45% of controls.

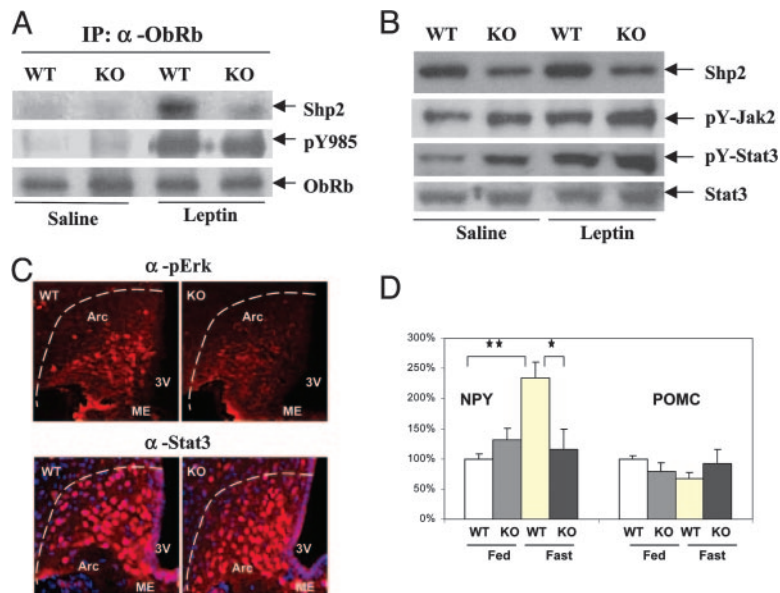


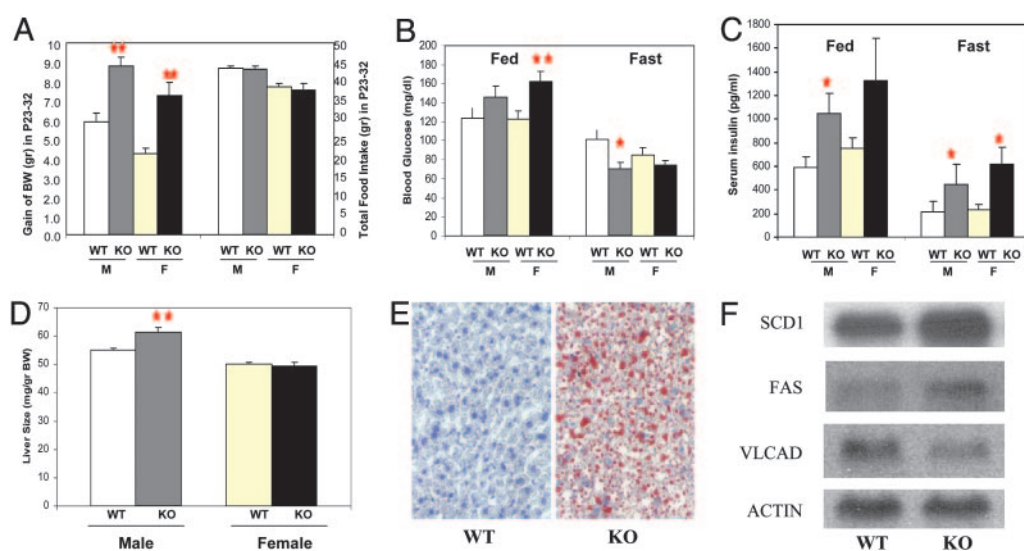
**Fig. 3.** Leptin-induced signals are directly interfered in CaSKO mice. (A–C) Mice at 8 weeks were fasted for 48 h and injected i.p. with leptin (100  $\mu$ g) or saline, and samples were taken after 15 min. (A) Hypothalamic lysates (1 mg total protein) were immunoprecipitated (IP) with an antibody against ObRb and blotted with antibodies recognizing pY985 of ObRb, Shp2, and ObRb. (B) Immunoblot analysis was performed by using antibodies for Shp2, pY-Jak2, pY-Stat3, and Stat3. For Stat3 or ObRb blotting, lysate containing 50  $\mu$ g protein was used, and for Shp2, 10  $\mu$ g protein was used. (C) Hypothalamic sections from leptin-treated control or CaSKO mice were immunostained with antibodies against phospho-Erk (Upper) or Stat3 (Lower). Third ventricle (3V), median eminence (ME), and arcuate nucleus (Arc) are indicated. (D) Eight-week-old mice were either fed ad libitum or fasted for 20 h before total RNA extraction from hypothalamus. Real-time RT-PCR was performed according to a previously published protocol (13). NPY, neuropeptide Y; POMC, proopiomelanocortin. \*\*,  $P < 0.01$ ; \*,  $P < 0.05$ . (Magnification: 100  $\mu$ M, C.)

min. This observation provides direct biochemical evidence for Shp2 being a signaling component for leptin in hypothalamus *in vivo* and also extends the previous *in vitro* data showing that Shp2 binds ObRb via phosphorylated Y985 in transfected 293 cells (8, 9). Ablation of Shp2 did not significantly affect the phosphorylation level of Y985, the Shp2 binding site on ObRb (Fig. 3A). Interestingly, both basal and leptin-induced tyrosine phosphorylation levels of Jak2 and Stat3 were modestly enhanced in the hypothalamus of CaSKO mice as compared with the controls (Fig. 3B), supporting the notion that Shp2 down-regulates the ObRb-Jak2/Stat3 pathway (8, 9). This idea is apparently at odds with the obese and hyperleptinemic phenotype of CaSKO mice, which strongly argues for a positive role of Shp2 in leptin signaling. To address this issue, we evaluated the leptin-induced Erk pathway in CaSKO mice. In contrast to the Jak2/Stat3 activation status, we demonstrate through immunohistochemical staining that leptin-induced phospho-Erk signals in the arcuate nucleus (ARC) of hypothalamus

were dramatically reduced in CaSKO mice compared with the control (Fig. 3C). Consistent with the immunoblot data in Fig. 3B, nuclear translocation of Stat3 was not impaired in the ARC upon leptin administration (Fig. 3C). Thus, despite a negative effect of Shp2 on Jak2/Stat3 activation, this phosphatase acts to promote leptin signaling, presumably through enhancing the Erk pathway, leading to hyperleptinemia in CaSKO mice.

Leptin induces the expression of anorexic gene products, such as proopiomelanocortin (POMC), and represses the expression of orexigenic peptides neuropeptide Y (NPY) and agouti-related protein (21, 22). RT-PCR analysis of hypothalamic signals downstream of the leptin receptor demonstrated no significant changes in the mRNA levels of *POMC* between control and CaSKO mice. However, the *NPY* mRNA level increased 2- to 3-fold in control mice after 20 h of fasting, with no increase detected in CaSKO mice (Fig. 3D), suggesting that Shp2 is required for leptin-induced inhibition of *NPY* expression independent of Stat3, which is consistent with previous observations (13).

**Fig. 4.** The obesity is caused primarily by altered metabolism. (A) After weaning, mice were followed daily for body weight (BW) and food intake. Gain of body weight within the 10-day period, from P23 to P32, differed significantly between control (WT) and CaSKO (KO) mice (\*\*,  $P < 0.0002$  with at least eight mice per group), whereas the food intake was equal between the two groups or even slightly less for CaSKO mice. M, male; F, female. (B and C) Blood glucose and serum insulin concentrations were measured for mice at 8 weeks, either fed or fasted for 20 h (\*,  $P < 0.05$ ; \*\*,  $P < 0.01$  with at least eight mice per group). (D) Liver samples were collected from 8-week-old mice. Data represent the relative liver weight versus body weight (mean  $\pm$  SEM) of at least eight mice for each gender and genotype (\*\*,  $P = 0.002$ ). (E) Mouse liver collected from 15-week-old mice was cryo-sectioned followed by staining with Oil-red-O and counterstaining with hematoxylin. Representative data from at least three independent pairs of littermates are shown. (F) Total RNAs were extracted from mouse liver at P28. The expression levels of stearoyl-CoA desaturase-1 (SCD1), fatty acid synthase (FAS), long chain acyl-CoA dehydrogenase (VLCAD), and actin were analyzed by Northern blotting following standard protocols. (Magnification: 50  $\mu$ M, E.)



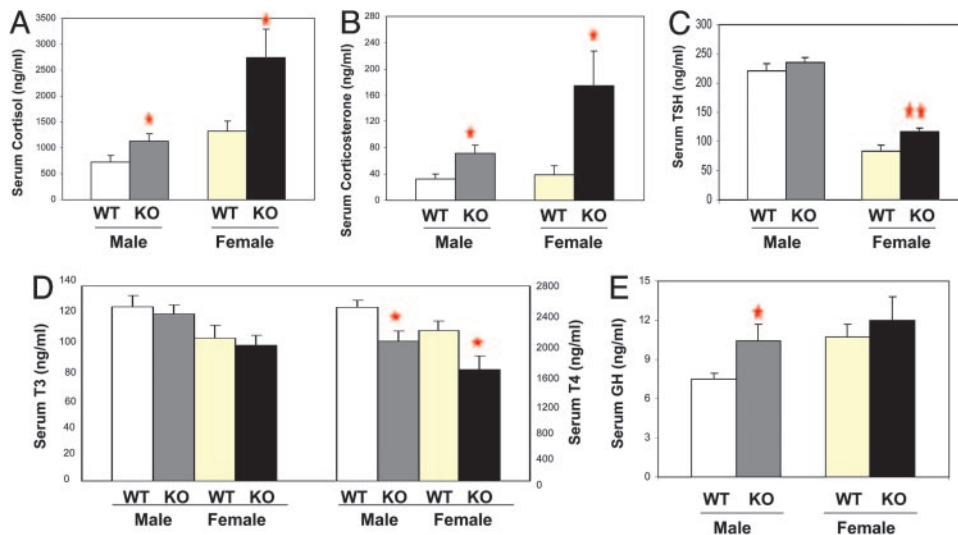


**Fig. 5.** Dysfunction of the hypothalamus-pituitary axis in CaSKO mice. Control and CaSKO mice ( $\approx 11$ – $13$  weeks old) were eyebled at 10–11 a.m. Adrenal hormone cortisol (A), pituitary hormones thyroid-stimulating hormone (TSH) (C) and GH (E), and thyroid hormones triiodothyronine (T3) and thyroxine (T4) (D) were determined by RIA. (B) Adrenal hormone corticosterone was measured by enzyme immunoassay; \*\*,  $P < 0.01$ ; \*,  $P < 0.05$ . There were at least eight mice in each group.

**CaSKO Mice Are Not Hyperphagic.** To explore the physiological mechanism for initiation of the obese phenotype, we assessed total food intake and body weight increase for the period of P23–32, a time window during which the onset of obesity occurs (Fig. 4A). At P23, the body weights of control and CaSKO mice were indistinguishable in both males and females. During the subsequent 10 days, CaSKO males gained 150% of body weight compared with controls and CaSKO females had a body weight increase at 172% of the controls ( $n \geq 8$  each group,  $P < 0.0002$ ), despite the fact that CaSKO mice consumed similar or even slightly reduced amounts of food compared with control animals (Fig. 4A). Therefore, CaSKO mice were not hyperphagic at the onset of obesity. We also compared food intake between control and CaSKO mice at 8 weeks of age, after the development of obesity, and found no significant difference (Table 1). Therefore, the obese phenotype of CaSKO mice was not caused by hyperphagia, but rather by alteration of metabolism upon deletion of *Shp2* in the brain. Consistently, the body temperature of CaSKO mice was significantly lower than the controls (35.8 versus 36.5°C, Table 1).

**CaSKO Mice Develop Diabetes and Fatty Liver.** We investigated glucose homeostasis and found that in the fed state CaSKO mice were hyperglycemic at 8 weeks of age (Fig. 4B). However, upon fasting for 20 h, the CaSKO mice became hypoglycemic compared to littermate controls (Fig. 4B). In contrast, hyperinsulinemia was detected in mutant mice in both the fed and fasting states (Fig. 4C). One plausible explanation for these results is that the *Shp2* mutation in CaSKO mice shifted metabolic pathways to favor anabolism over catabolism, resulting in decreased blood glucose under fasting conditions/stress.

Although the size and weight of most organs, such as heart, kidney, and spleen, appeared normal in CaSKO mice (Fig. 7, which is published as supporting information on the PNAS web site), the liver size in male mutants was significantly increased by 12% ( $P = 0.002$ , Fig. 4D). Oil-red-O staining on cryo-sections from 15-week-old CaSKO mice detected fatty liver (Fig. 4E). In addition to fat storage within hepatic cells, characteristic of fatty liver, triglycerides were secreted from hepatocytes but were abnormally accumulated in the liver, contributing to the hepatomegaly phenotype. Indeed, periodic acid-Schiff staining displayed elevated glycogen deposits in CaSKO livers (data not shown). Female CaSKO mice also developed enlarged and steatotic liver, to a lesser extent than males (data not shown). Thus, deletion of *Shp2* in the CNS resulted in drastic hepatic glucose/lipid metabolic alterations, as in *ob/ob* and *db/db* as well as *Stat3<sup>N-/-</sup>* mutant mice (4, 14).

Little is known about the role of leptin in the control of

metabolism, which is distinct from its anorectic effect (23, 24). A recent report suggests a mechanism for leptin's metabolic action by down-regulating stearoyl-CoA desaturase-1 (SCD-1) expression in the liver (7). To assess the expression of genes controlling lipid metabolism in the liver, total RNAs were extracted from CaSKO mouse livers at the age of P28 (at the onset of obesity). Northern blot analysis demonstrated that expression of lipogenic genes, such as SCD-1 and fatty acid synthase, was up-regulated, whereas a lipolytic gene coding for very long chain acyl-CoA dehydrogenase was down-regulated (Fig. 4F). As these changes were detected before the development of obesity, such altered expression of the enzymes is unlikely the consequence of metabolic disorders in mutant animals.

**CaSKO Mice Exhibit Defects in the Hypothalamus-Pituitary Axis.** Leptin-initiated signals in the hypothalamus act through pituitary hormones to control metabolism, and leptin-deficient *ob/ob* mice display severe dysfunctions in the hypothalamus-pituitary axis (4). CaSKO mice exhibited hypersecretion of glucocorticoids such as cortisol and corticosterone (Fig. 5A and B). Consistent with the *ob/ob* phenotype, CaSKO female mice at  $\approx 13$ – $15$  weeks of age had higher serum levels of thyroid-stimulating hormone levels (Fig. 5C), with modestly decreased serum triiodothyronine and significantly lower thyroxine levels (Fig. 5D) (25). Compared with controls, CaSKO mice displayed increased linear growth, expressed as the snout-anus length (Table 1) and, consistently, hypersecretion of GH was observed in male mutants and to the lesser extent in female mutants (Fig. 5E). In *ob/ob* and *Stat3<sup>N-/-</sup>* mice, GH is hyposecreted and the snout-anus length is shorter than in WT animals. Finally, CaSKO mice displayed severe impairment in reproduction (45% breeding efficiency, Table 1), whereas *ob/ob* mice were completely sterile.

## Discussion

In this study, we have created a conditional mutant allele of *Shp2* in mice and uncovered a critical role of *Shp2* in energy homeostasis in adult mammals, by deleting *Shp2* in postmitotic CNS neurons. A prominent phenotype of CaSKO mice was the development of early-onset obesity, and this obese phenotype naturally guided us into the leptin system.

Previous *in vitro* experiments suggested negative or positive roles of *Shp2* in leptin signaling, presumably through down-regulation of Jak2/Stat3 activity or promotion of the Erk pathway (8, 9, 26). Affinity chromatography using a tyrosine phosphorylated peptide modeled on Tyr-985 of ObRb resulted in isolation of *Shp2* as its binding partner from bovine and mouse hypothalamus (9). In

cotransfection experiments of 293T cells, physical association of Shp2 with ObRb was shown to correlate with a decreased phosphorylation of Jak2 induced by leptin (9). Another group showed that mutation of this tyrosine site on ObRb resulted in disruption of Shp2 tyrosine phosphorylation and binding to the receptor and up-regulation of gene induction mediated by Stat3 in cell lines (8). Interestingly, Tyr-985 has also been shown to bind Socs3, another negative regulator of Jak2/Stat3 signals (27). Deletion of Socs3 in the brain leads to prolonged Stat3 activation in the hypothalamus by leptin, elevated leptin sensitivity, and resistance to diet-induced obesity; a similar phenotype was observed in Socs3<sup>+/-</sup> mice (28, 29).

By using a tissue-specific gene targeting approach, we have demonstrated that Shp2 indeed acts to suppress Jak2/Stat3 activation by leptin and simultaneously promote the leptin-induced Erk pathway in the hypothalamus. More importantly, the combined genetic and biochemical analyses *in vivo* illustrates a notion that the positive effect of Shp2 outweighs its negative role in leptin-elicited signaling pathways. Overall, Shp2 tyrosine phosphatase appears to enhance leptin signals, evidenced by the obese and hyperleptinemic phenotype in CaSKO mice. Another tyrosine phosphatase, PTP-1B, has been shown to act primarily as a negative effector in leptin signaling in the hypothalamus through dephosphorylating Jak2, and crossing of *ob/ob* mice with PTP1B KOs alleviated the obesity and metabolic disorders in the leptin-deficient mice (30, 31).

The requirement of Stat3 for leptin signaling through ObRb in hypothalamus for control of energy balance has been well documented (12–14). In this regard, it is interesting to note that development of obesity in CaSKO mice occurs when Stat3 is highly activated by leptin in the hypothalamus. This finding may explain some disparities between *ob/ob* and CaSKO phenotypes. Hypersecretion of GH was observed in CaSKO mice with increased linear growth (particularly in males), as compared with hyposecretion of GH in *ob/ob* mice with shortened snout-anus length. The reproductive capacity in CaSKO mice was impaired but not completely blocked as in *ob/ob* mice, suggesting residual leptin signals in the absence/decrease of Shp2. Further comparative analyses of hypothalamic signaling defects in *ob/ob*, Stat3<sup>N-/-</sup>, and CaSKO mice will help to elucidate the molecular mechanism for leptin action in control of energy balance.

Unlike many other animal models available, development of obesity is not accompanied by hyperphagia in CaSKO mice. On the other hand, CaSKO mice developed fatty liver, as in *ob/ob* mice, suggesting that Shp2 is a pivotal mediator of leptin's metabolic

effect. Although mostly known for its anorectic activity, leptin can notably stimulate a metabolic response. Administration of leptin into *ob/ob* mice and humans leads to reduction of lipid in liver and adipose tissues and improves insulin sensitivity (23, 24, 32–35). Consistent with a recent report (7), this study suggests Shp2 is a critical component in transducing the metabolic signal of leptin through control of stearoyl-CoA desaturase-1 expression in the liver. Obviously, the CaSKO mouse will be an ideal model for dissection of the physiological pathway for leptin's metabolic action.

This study defines a critical function of Shp2 in the brain control of body weight, glucose homeostasis, and energy balance in adult mammals. Evidently, the obese phenotype of CaSKO mice is significantly contributed by disruption of hypothalamic leptin signaling. The CaSKO mice recapitulated many aspects of the *ob/ob* and *db/db* phenotypes and, in particular, initiation of obesity in all of these mutant mice coincides at P28, a time point for onset of leptin signaling in energy homeostasis. Deletion of insulin receptor in neural stem cells (that give rise to all neuronal and glial cells) mediated by nestin-Cre caused no obesity in male animals within 6 months (18), whereas severe obesity developed in CaSKO mice in which Shp2 was deleted in postmitotic CNS neurons. This striking difference argues that the onset of obesity in CaSKO mice is not related to suppression, if any, of insulin signals by Shp2 deletion, although disturbed insulin signaling may be part of the metabolic disorders in aged mutant mice. In preliminary experiments, normal *BDNF* transcript levels were detected in CaSKO mice. However, a detailed functional analysis is needed to determine whether Shp2 deletion in the brain alters *BDNF* signaling, which consequently contributes to the obese phenotype.

In summary, although we clearly need to further investigate the possibility that other signaling defects may also contribute to the obese phenotype of the CaSKO animals, the data presented indicate a prominent role for defective leptin receptor signaling in the development of obesity in these mice. Therefore, we propose that pharmaceutical augmentation of Shp2 activity in the brain may potentially be an efficient therapeutic strategy for alleviation of leptin resistance in obese patients.

We thank Dr. S. Zeitlin (Columbia University, New York) for the CaMKII $\alpha$ -Cre mice, Dr. R. T. Premont (Duke University, Durham, NC) for the triple-loxP vectors, and our colleagues for stimulating discussion. This work was supported by National Institutes of Health Grant R01GM53660 (to G.-S.F.). G.-S.F. was a recipient of a career development award from the American Diabetes Association.

- Lai, L. A., Zhao, C., Zhang, E. E. & Feng, G. S. (2003) in *Protein Phosphatases*, eds. Arino, J. & Alexander, D. (Springer, Berlin), Vol. 5, pp. 275–299.
- Neel, B. G., Gu, H. & Pao, L. (2003) *Trends Biochem. Sci.* **28**, 284–293.
- Saxton, T. M., Henkemeyer, M., Gasca, S., Shen, R., Rossi, D. J., Shalaby, F., Feng, G. S. & Pawson, T. (1997) *EMBO J.* **16**, 2352–2364.
- Zhang, Y., Proenca, R., Maffei, M., Barone, M., Leopold, L. & Friedman, J. M. (1994) *Nature* **372**, 425–432.
- Flier, J. S. (2004) *Cell* **116**, 337–350.
- Friedman, J. M. & Halaas, J. L. (1998) *Nature* **395**, 763–770.
- Cohen, P., Miyazaki, M., Succi, N. D., Hagge-Greenberg, A., Liedtke, W., Soukas, A. A., Sharma, R., Hudgins, L. C., Ntambi, J. M. & Friedman, J. M. (2002) *Science* **297**, 240–243.
- Carpenter, L. R., Farruggella, T. J., Symes, A., Karow, M. L., Yancopoulos, G. D. & Stahl, N. (1998) *Proc. Natl. Acad. Sci. USA* **95**, 6061–6066.
- Li, C. & Friedman, J. M. (1999) *Proc. Natl. Acad. Sci. USA* **96**, 9677–9682.
- Ghilardi, N., Ziegler, S., Wiestner, A., Stoffel, R., Heim, M. H. & Skoda, R. C. (1996) *Proc. Natl. Acad. Sci. USA* **93**, 6231–6235.
- Baumann, H., Morella, K. K., White, D. W., Dembski, M., Bailon, P. S., Kim, H., Lai, C. F. & Tartaglia, L. A. (1996) *Proc. Natl. Acad. Sci. USA* **93**, 8374–8378.
- Vaisse, C., Halaas, J. L., Horvath, C. M., Darnell, J. E., Jr., Stoffel, M. & Friedman, J. M. (1996) *Nat. Genet.* **14**, 95–97.
- Bates, S. H., Stearns, W. H., Dundon, T. A., Schubert, M., Tso, A. W., Wang, Y., Banks, A. S., Lavery, H. J., Haq, A. K., Maratos-Flier, E., et al. (2003) *Nature* **421**, 856–859.
- Gao, Q., Wolfgang, M. J., Neschens, S., Morino, K., Horvath, T. L., Shulman, G. I. & Fu, X. Y. (2004) *Proc. Natl. Acad. Sci. USA* **101**, 4661–4666.
- Dragatsis, I. & Zeitlin, S. (2000) *Genesis* **26**, 133–135.
- Rios, M., Fan, G., Fekete, C., Kelly, J., Bates, B., Kuehn, R., Lechan, R. M. & Jaenisch, R. (2001) *Mol. Endocrinol.* **15**, 1748–1757.
- Soriano, P. (1999) *Nat. Genet.* **21**, 70–71.
- Bruning, J. C., Gautam, D., Burks, D. J., Gillette, J., Schubert, M., Orban, P. C., Klein, R., Krone, W., Muller-Wieland, D. & Kahn, C. R. (2000) *Science* **289**, 2122–2125.
- Kernie, S. G., Liebl, D. J. & Parada, L. F. (2000) *EMBO J.* **19**, 1290–1300.
- Xu, B., Goulding, E. H., Zang, K., Cepoi, D., Cone, R. D., Jones, K. R., Tecott, L. H. & Reichardt, L. F. (2003) *Nat. Neurosci.* **6**, 736–742.
- Cowley, M. A., Smart, J. L., Rubinstein, M., Cerdan, M. G., Diano, S., Horvath, T. L., Cone, R. D. & Low, M. J. (2001) *Nature* **411**, 480–484.
- Schwartz, M. W., Woods, S. C., Porte, D., Jr., Seeley, R. J. & Baskin, D. G. (2000) *Nature* **404**, 661–671.
- Kamohara, S., Burcelin, R., Halaas, J. L., Friedman, J. M. & Charron, M. J. (1997) *Nature* **389**, 374–377.
- Levin, N., Nelson, C., Gurney, A., Vandlen, R. & de Sauvage, F. (1996) *Proc. Natl. Acad. Sci. USA* **93**, 1726–1730.
- York, D. A., Otto, W. & Taylor, T. G. (1978) *Comp. Biochem. Physiol. B* **59**, 59–65.
- Bjorbaek, C., Buchholz, R. M., Davis, S. M., Bates, S. H., Pierroz, D. D., Gu, H., Neel, B. G., Myers, M. G., Jr., & Flier, J. S. (2001) *J. Biol. Chem.* **276**, 4747–4755.
- Bjorbaek, C., Lavery, H. J., Bates, S. H., Olson, R. K., Davis, S. M., Flier, J. S. & Myers, M. G., Jr. (2000) *J. Biol. Chem.* **275**, 40649–40657.
- Mori, H., Hanada, R., Hanada, T., Aki, D., Mashima, R., Nishinakamura, H., Torisu, T., Chien, K. R., Yasukawa, H. & Yoshimura, A. (2004) *Nat. Med.* **10**, 739–743.
- Howard, J. K., Cave, B. J., Oksanen, L. J., Tzamelis, I., Bjorbaek, C. & Flier, J. S. (2004) *Nat. Med.* **10**, 734–738.
- Zabolotny, J. M., Bence-Hanulec, K. K., Stricker-Krongrad, A., Haj, F., Wang, Y., Minokoshi, Y., Kim, Y. B., Elmquist, J. K., Tartaglia, L. A., Kahn, B. B. & Neel, B. G. (2002) *Dev. Cell* **2**, 489–495.
- Cheng, A., Uetani, N., Simoncic, P. D., Chaubey, V. P., Lee-Loy, A., McGlade, C. J., Kennedy, B. P. & Tremblay, M. L. (2002) *Dev. Cell* **2**, 497–503.
- Halaas, J. L., Gajiwala, K. S., Maffei, M., Cohen, S. L., Chait, B. T., Rabinowitz, D., Lallone, R. L., Burley, S. K. & Friedman, J. M. (1995) *Science* **269**, 543–546.
- Pelleymounter, M. A., Cullen, M. J., Baker, M. B., Hecht, R., Winters, D., Boone, T. & Collins, F. (1995) *Science* **269**, 540–543.
- Shimomura, I., Hammer, R. E., Ikemoto, S., Brown, M. S. & Goldstein, J. L. (1999) *Nature* **401**, 73–76.
- Farooqi, I. S., Matarese, G., Lord, G. M., Keogh, J. M., Lawrence, E., Agwu, C., Sanna, V., Jebb, S. A., Perna, F., Fontana, S., et al. (2002) *J. Clin. Invest.* **110**, 1093–1103.